2016-11-15

Quantum Dot Band Gap Investigations

John Ryan Peterson
Brigham Young University - Provo, jryan388@gmail.com

The author worked with Dr. John S. Colton in the BYU Physics department on this project. This was part of the BYU REU program. The National Science Foundation funds undergraduate research across the country through the REU program.

Quantum Dot Band Gap Investigations

J. Ryan Peterson

Thanks to: Dr. John S. Colton (advisor)

Kameron Hansen, Luis Perez, Cameron Olsen

Abstract

Improving solar panel efficiency has become increasingly important as the world searches for cheap renewable energy. Recent developments in the industry have focused on multi-layer cells, some of which use semiconducting dyes to absorb light in place of crystalline solids. In this paper, I characterize various dyes recently synthesized for use in solar panels. These dyes contain semiconducting nanoparticles enclosed primarily by the protein ferritin to limit particle size. The band gaps were measured using either optical absorption spectroscopy or measuring the photoluminescence spectrum, depending on the type of semiconductor. The results indicate that both manganese oxide and lead sulfide nanoparticles can be synthesized in ferritin and their band gaps tuned to slightly above and below 1 eV. In addition, it was shown that ferritin effectively protects against the photocorrosion which is common when particles are synthesized without its protection.

Introduction

Efficiencies of single-junction solar cells have risen over the years, but are now reaching their performance ceiling due to the Shockley-Queisser Limit of 33.7% efficiency. In order to raise efficiency, materials with varying band gaps must be used in multi-junction cells. These cells can capture more energy from the solar spectrum than any one material alone. One approach to this type of cell is using semiconducting dyes to absorb the photons. Our lab has investigated the use of the protein ferritin as a template for synthesizing nanoparticles or quantum dots in these dyes [1].

The key to varying the band gaps of the quantum dots is varying the radii in a controlled manner. This is done by controlling the concentration of reactants used to synthesize the nanoparticles. When the radius of a quantum dot is sufficiently small (a few nanometers), quantum confinement of the electron wave function limits the energy of valence electrons according to the Brus Equation:

$$E(r) = E_{gap} + \frac{h^2}{8r^2}\left(\frac{1}{m_e} + \frac{1}{m_h}\right), \quad (1)$$

where E_{gap} is the band gap of the semiconductor in bulk, and m_e and m_h are the effective electron and hole masses, respectively. As the radius r become smaller, the second term becomes more significant and raises the band gap above that of the semiconductor in bulk. Because of the assumptions made to simplify this equation, it can only approximately predict the band gaps for nanoparticles with radii that are neither too large or small, however, it can provide radii to target when seeking specific band gaps.

In our lab, we have synthesized these quantum dots inside the protein ferritin. Ferritin is a spherical protein traditionally used by the body to store and transport iron. By removing the iron core, a spherical cavity 8 nm in diameter is left, which can be used as a template for synthesizing other nanoparticles.

Materials and Methods

Optical absorption spectroscopy was used to measure the band gap of the manganese and cobalt oxide core ferritin solutions, as they are indirect band gap semiconductors. Broadband light from a xenon arc lamp was directed into a monochromator to select individual wavelengths. Then the light passed through a chopper to allow lockin detection for increased signal-to-noise, after which it passed through a cuvette and into a silicon photodiode detector. A cuvette filled with TRIS buffer solution was used as a control, after which another cuvette containing metal oxide core ferritin suspended in the same buffer solution was used. The intensities of the light through the control solution and the ferritin solution were measured at 2nm intervals to obtain the transmission. The absorption coefficient was calculated as the negative log of the transmission, and the square root plotted over energy. The indirect band gap was found by fitting a line to the square root of the absorption coefficient and solving for the x-intercept according to the following equation:

$$\sqrt{\alpha} \sim \hbar\omega - E_{ig}. \quad (2)$$

As direct transitions are often possible at higher energies, the direct band gaps of indirect band gap materials were found by fitting a similar equation and solving for the x-intercept:

$$\sqrt{\alpha} \sim \hbar\omega - E_{ig}. \quad (3)$$

We have omitted the phonon energy in these equations as it was negligible in our samples.

The band gaps of the manganese and cobalt core ferritin samples were initially measured only a few day after synthesis using a xenon arc lamp. However, the spectrum of the xenon lamp prevented its use past 810 nm in reasonable intervals of time with a lockin amplifier. It appeared that the absorption plateaued at 700 to 800 nm. We assumed that this was due to some non-wavelength-dependent

scattering, and therefore normalized the entire absorption curve to the absorption at approximately 700 nm. Our later acquisition of a tungsten halogen lamp provided us with a much smoother spectrum, which showed that absorption is actually still increasing at longer wavelengths in both of these samples. Unfortunately, the samples had changed character in the several months that they had been sitting in our lab at room temperature, showing radically different trends in the band gaps. We decided to use the previous data taken with the xenon arc lamp, which we then renormalized because of the information obtained about longer-wavelength absorption.

For direct band gap materials, photoluminescence was measured to determine the band gap. As the lead sulfide samples were expected to have a band gap close to 1 eV, a 398nm Thorlabs diode laser was used to excite photoluminescence. The samples were dried on microscope slides, and the sample was illuminated with the laser at 100 mW, which was modulated at 5 kHz in order to use lockin detection. The photoluminescent light was focused into a Digikrom DK240 spectrometer, after which a LN-cooled Teledyne Judson J16D germanium photodiode detector was used to measure intensity. The resulting spectrum was divided by the detector's efficiency (obtained from Teledyne Judson) to correct for nonlinear response. The spectrometer has much more uniform response at our wavelengths of interest than the detector, so it was not taken into account.

Results

Optical absorption spectroscopy conducted on the manganese core ferritin solutions revealed multiple absorption edges, as shown in Figure 1:

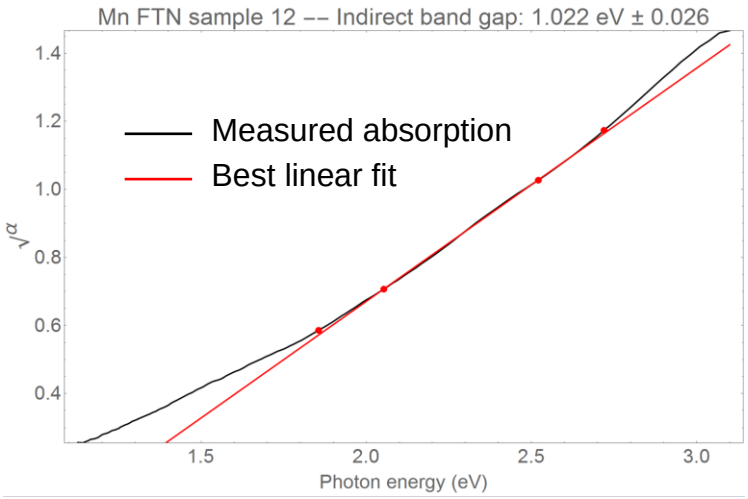

Figure 1: The indirect absorption plots revealed an absorption edge lower than the section which was used for the linear fit.

One possible explanation for this nonlinear low-energy absorption on the indirect band gap scan was scattering. However, after measuring the scattered light intensity by placing a detector to the side of the cuvette and measuring intensity at every wavelength, we found that even at 3 eV, less than 5% of the incoming light is scattered instead of absorbed. Much less than that was absorbed at the low energies we were interested in. We decided that the most likely explanation for this behavior was defect binding, as the lower absorption edge did not continue linearly and gave way to the second edge. We fit a line to this second edge to determine the band gap. This defect behavior has been seen before in ferritin-enclosed nanoparticles, namely iron core ferritin synthesized previously by our group [2].

The optical absorption spectroscopy revealed indirect band gaps for the manganese oxide core ferritin samples between 1.01 eV and 1.34 eV, as listed in Table 1. However, some absorption was present even at lower energies than the band gap listed here. We attribute this to the fact that the band gap we report is only the center of a distribution of band gaps due to the distribution of nanoparticle sizes, and some of the nanoparticles will have a band gap lower than the average. In addition, the defect binding previously discussed contributed to low-energy absorption.

Table 1: Band gap results for Manganese oxide nanoparticles in ferritin, synthesized using various combinations of manganese and permanganate. The pH at which the synthesis was conducted, as well as the presence of oxygen, are listed for each sample. Samples 9 and 10 are not listed, as their band gaps could not be measured due to insufficient core size.

Sample	Ratio of Mn^{II}:MnO_4^-	Aerobic?	pH	Indirect Gap (eV)	Indirect Error (eV)	Direct Gap (eV)	Direct Error (eV)
1	0	No	5.4	1.34	0.07	2.69	0.02
2	3:2	No	5.4	1.26	0.08	2.66	0.01
3	2:1	No	5.4	1.21	0.09	2.64	0.01
4	4:1	No	5.4	1.17	0.09	2.63	0.01
5	0	Yes	5.4	1.30	0.08	2.70	0.05
6	3:2	Yes	5.4	1.21	0.09	2.68	0.02
7	2:1	Yes	5.4	1.23	0.08	2.68	0.02
8	4:1	Yes	5.4	1.19	0.10	2.64	0.02
11	3:2	No	9.4	1.10	0.05	2.56	0.02
12	2:1	No	9.4	1.05	0.05	2.80	0.03
13	4:1	No	9.4	1.09	0.05	2.99	0.03
14	0	Yes	9.4	1.30	0.09	2.72	0.01
15	3:2	Yes	9.4	1.21	0.05	2.56	0.02
16	2:1	Yes	9.4	1.16	0.07	2.65	0.02
17	4:1	Yes	9.4	1.19	0.05	2.52	0.02
18	1:0	Yes	9.4	1.01	0.05	2.51	0.01

Band gaps for the Co:Mn comproportionation samples also had higher-wavelength absorption than previously thought, because of which their normalization was removed as well. The new results show indirect band gaps ranging from about 0.6 eV to 1.0 eV, as seen in Figure 2 below.

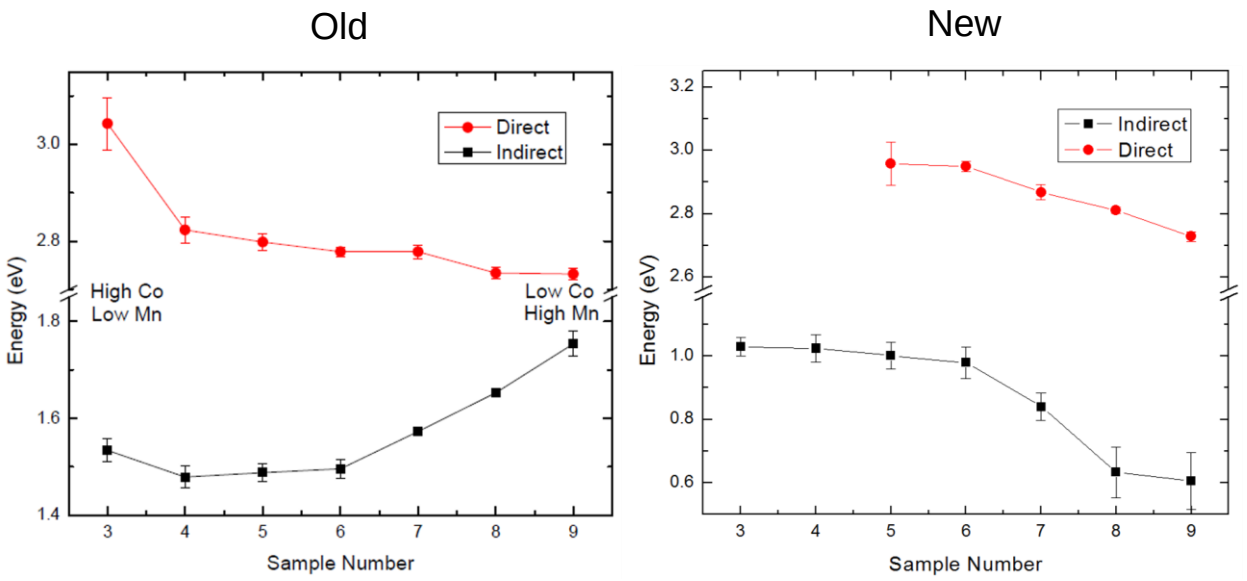

Figure 2: Comparison of the band gaps previously accepted for the Co:Mn comproportionation samples compared to the new band gaps obtained after adjusting the normalization. Samples are listed in order of increasing manganese fraction. Direct band transition energies are not reported for samples 3 and 4 as their direct absorption plots were not linear.

Photoluminescence measured from the PbS ferritin samples showed direct band gaps from just under 1.0 eV to about 1.3 eV. Samples were synthesized in oxygen and nitrogen environments; the band gaps of the oxygen samples are listed in Table 2 below. Samples with the largest cores appeared to have band gaps lower than any of those listen in Table 2, but the germanium detector used to measure photoluminescence was not able to measure sufficiently low-energy light to determine the band gaps.

Table 2: Band gaps measured on samples synthesized in an oxygen environment. The samples are listed in order of increasing reactant concentration and thus increasing core size.

PbS FTN Samples	Direct gap (eV)	FWHM (eV)
Aerobic Sample 1	1.33	0.33
Aerobic Sample 2	1.31	0.35
Aerobic Sample 3	1.14	0.31
Aerobic Sample 4	1.12	0.3
Aerobic Sample 5	1.06	0.29
Aerobic Sample 6	0.93	0.32

The radii for several of the lead sulfide ferritin samples were measured as well. The expected band gaps based on these radii were calculated and compared to the measured band gaps in Table 3 below. The expected and measured band gaps matched well for the nanoparticles with radii near 3 nm, but the effect on band gap of a radius smaller or larger than 3 nm was less than expected.

Table 3: After measuring core sizes of several samples on the transmission electron microscope, the expected band gaps, predicted using the measured radii and Equation 1, are compared with the band gaps measured using photoluminescence

PbS FTN Samples	**Measured Radius**	**Expected Band Gap (Brus equation)**	**Measured Band Gap and FWHM**
Aerobic Sample 1	2.25 ± 0.48 nm	1.70 eV (1.29 eV - 2.50 eV)	1.33 eV (0.33 eV)
Aerobic Sample 3	3.03 ± 0.39 nm	1.12 eV (.97 eV – 1.35 eV)	1.14 eV (0.31 eV)
Anaerobic Sample 3	3.04 ± 0.54 nm	1.12 eV (.92 eV – 1.46 eV)	1.23 eV (0.23 eV)
Anaerobic Sample 6	5.70 ± 0.89 nm	0.61 eV (.56 eV - .69 eV)	1.0 eV (0.3 eV)
Aerobic Sample 6	6.10 ± 0.89 nm	0.59 eV (.54 eV - .65 eV)	< 1.0 eV

Some samples in our lab were synthesized without the use of ferritin. Thioglycerol was used with these lead sulfide samples to limit nanoparticle growth in solution after they had reached the desired radii. The radii and band gaps of these samples were successfully tuned just as the ferritin-based nanoparticles were. However, even after a short period of time, exposure to light caused these samples to degrade, unlike the nanoparticles synthesized inside ferritin. They showed both an increase in peak photoluminescence intensity as well as a shift to higher-energy emission, as shown in Figure 3 below.

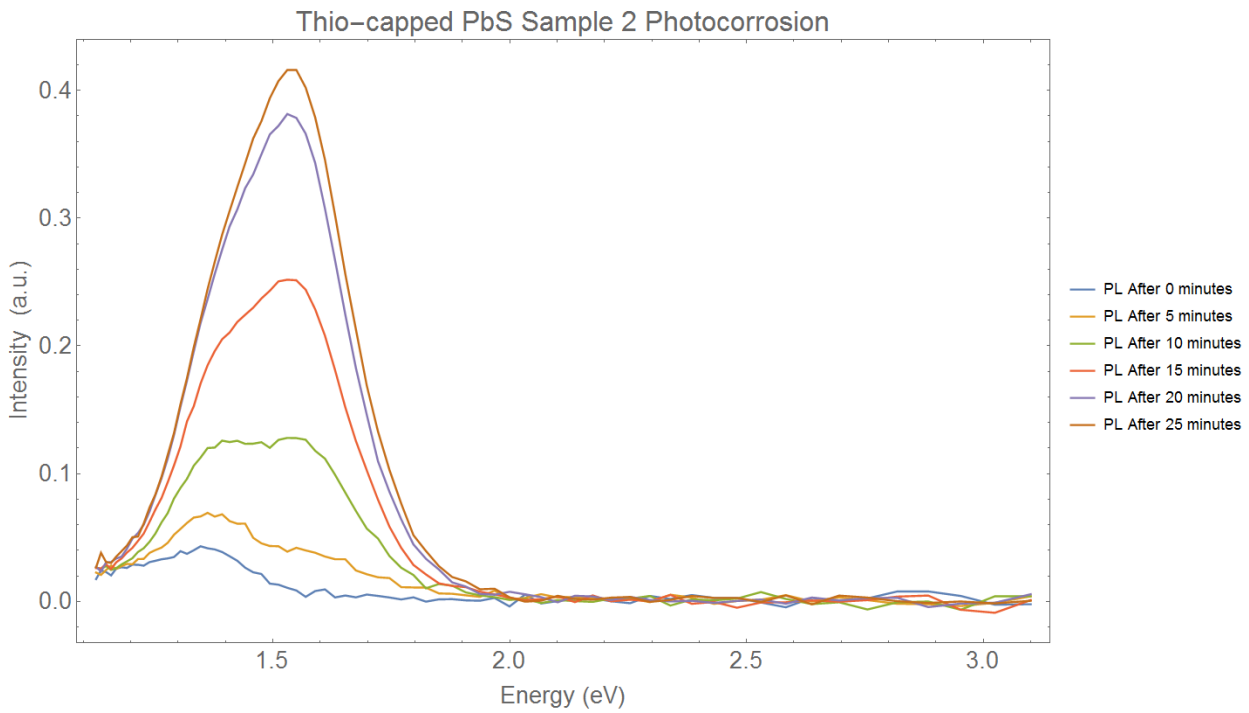

Figure 3: Photocorrosion in non-ferritin lead sulfide is shown by a shifting band gap as the sample is exposed to light. Photoluminescence spectra were measured every five minutes after exposure to the laser.

Discussion

The manganese ferritin band gaps show a strong trend of increasing band gap with increasing permanganate concentration. In addition, the presence of oxygen only minimally lowered the band gaps of the acidic samples, but the basic samples appear significantly lower when synthesized in oxygen. The data shows that the band gap can be precisely tuned by controlling for reactant concentration, pH, and presence of oxygen to synthesize any arbitrary band gap in the range shown.

The indirect band gap results for the manganese and cobalt comproportionation samples show a reversed trend as the manganese fraction increases in comparison to the old data. However, the fact that a consistent trend exists, even if in the opposite direction, means that any arbitrary band gap within the range can be easily targeted.

The combined use of manganese-permanganate and cobalt-manganese comproportionation allows targeting of any band gap between about 0.6 eV and 1.3 eV. This wide range would allow us to create multiple layers for a multi-junction solar cell in this band gap range, increasing efficiency. However, as both the manganese-permanganate and cobalt-manganese samples are indirect band gap semiconductors, the required thickness could be prohibitive.

An alternative to using indirect band gap semiconductors could be lead sulfide, which is direct and would absorb much more light. Our efforts to vary nanoparticle size also reached up to 1.3 eV, but it is unclear if they could reach as low as the indirect band gap nanoparticles due to the detector responsitivity. Future work could include obtaining a new detector sensitive enough to measure photoluminescence at longer wavelengths to determine the lower limit on our lead sulfide nanoparticle band gaps. However, a band gap of 1.1 eV, which we have synthesized successfully, would be very effective when combined with other materials previously synthesized by our group and may be all that is needed [3].

The measured lead sulfide band gaps listed in Table 3 appear to diverge somewhat from the expected band gaps, but generally remain within the error bounds. Equation 1 will not hold perfectly, as our nanoparticles may not be entirely spherical and the approximation breaks down for smaller nanoparticles [4]. In order to determine what concentrations of reactants to use to achieve a specific band gap, it would be more effective to synthesize a collection of various sizes of nanoparticles and then measure the band gaps, as we have also done.

The photocorrosion shown in Figure 3 is significant cause for concern when creating solar cells with non-ferritin-based quantum dots. The change in photoluminescence means that there is a change in core composition as the nanoparticles are exposed to light. While it is not immediately clear what reactions are taking place, the fact that the band gap changes is concerning. Achieving high efficiency

with a multi-junction solar cell requires carefully selecting the band gaps of each layer to maximize the amount of energy obtained. However, if the band gaps of these substances change when exposed to light, the efficiency could be negatively affected. Fortunately, ferritin very effectively prevented this in the vast majority of our samples.

Future work will involve measuring the band gaps of new samples of lead sulfide or other nanoparticles inside ferritin, as well as working to measure the photoluminescence of the largest lead sulfide nanoparticles with a new detector. We hope to improve deposition techniques for our solar cells and then begin work on fabricating multi-junction cells in our lab.

Bibliography

[1] T. J. Smith, S. D. Erickson, C. M. Orozco, A. Fluckiger, L. M. Moses, J. S. Colton, and R. K. Watt, J. Mater. Chem. A **2**, 20782 (2014).

[2] J. S. Colton, S. D. Erickson, T. J. Smith, and R. K. Watt, Nanotechnology **25**, 135703 (2014).

[3] S. D. Erickson, T. J. Smith, L. M. Moses, R. K. Watt, and J. S. Colton, (2015).

[4] E. O. Chukwuocha, M. C. Onyeaju, and T. S. T. Harry, World J. Condens. Matter Phys. **2**, 96 (2012).